

Supporting Information

Random nanocrack assisted metal nanowire bundled network fabrication for a highly flexible and transparent conductor

By Young D Suh¹†, Sukjoon Hong¹†, Jinhwan Lee¹, Habeom Lee¹, Seongmin Jung¹, Jinhyeong Kwon¹, Hyunjin Moon¹, Phillip Won¹, Jaeho Shin¹, Junyeob Yeo², Seung Hwan Ko¹*

S1. Size distribution of random crack

The depth can be controlled by wet etching of cracked silicon substrate. As shown in Figure 2b, the initial nano cracks²⁶ (ranging from 100 to 150nm) are wet-etched to obtain various channel widths ranging from several hundreds of nanometers up to tens of micrometers. Since the diluted HNA solution is used, the etch width is the control factor: typically, two times of the depth²³. This can be verified by the typical cross section image (bottom right) of the replicated template shown in supplementary Figure S3. The diluted HNA solution is also advantageous in terms of controlling the etch width since the reaction rate is much slower than that of the undiluted solution. The geometry of conducting material including the channel width and depth of the master mold affects the optical and electrical properties of the transparent conductor film. We find that 7 μm width with high density cracks yields to ~85% transmittance which is comparable to other reported studies using random fracture. For simplicity, the channel width is fixed at 7 μm for the transmittance and sheet resistance measurement between the samples with different grid sizes. There is a slight variation in the crack width. The initial crack width varies from 100 nm to 180 nm. However, the channel width of the master mold after wet etching has much less variation since the scale is greatly increased compared to initial nanometer scale crack width. To confirm this, an inverse of master mold is thoroughly inspected as shown in supplementary Figure S3. The inverse master mold is divided into 8 different sections, and three arbitrary

locations of the corresponding sections are examined by SEM image. The width average is 8.46 μm and the standard deviation is 0.499 μm .

S2. Blading for complete removal of Ag NW residues

In order to maintain clean top surface of the mold for the quality of TC, additional blading is required after the Ag NW solution is dried. The Ag NW residues often remain on the top surface of the mold as shown in supplementary Figure S4b when the Ag NW solution is casted. Successive blading completely removes these residues as shown in supplementary Figure S4a. To verify complete removal of the residues, a BANN-based TC sample is inspected by a high magnification SEM image and a corresponding EDS map showing Ag peaks as shown in supplementary Figure S4c and S4d.

S3. Comparison between embedded nanowire networks by bar-coating method and BANN-based TC fabrication method

Bar coating method is comparably simple in terms of fabrication process. Two embedded bar-coated samples using equal amount of Ag NW (5-10 μm length with 45-50 nm diameter) dispersed solution (0.1 wt%) and 2x amount of Ag NW as shown in supplementary Figure S2a. With 1 ml of the Ag NW solution, we were unable to fabricate a conducting sample using bar-coating method even on a smaller substrate than that of BANN-based TC sample. To fabricate a conducting sample over 2 x 4 cm area, more than 2 ml of Ag NW solution must be used yet coagulation often occurs thus sheet resistance varies at such locations. On the other hand, controlled casting of Ag NW bundles selectively in the crack openings achieves higher

transmittance at given nanowire solution amount. Figure of merit (FoM) for BANN and bar-coated embedded NW network are 28.4 and 58.8 respectively.

S4. Sheet resistance uniformity of BANN-based TC

The sheet resistance uniformity of a BANN-based TC (4-inch wafer scale) sample as shown in supplementary Figure S2a and S2b was measured. The result shows slight sheet resistance variation between 80 and 110 ohm/sq. For high resolution resistive touch screen panel application, this can be improved by reducing average grid size which is directly related to crack density. The crack density can be increased by inducing higher stress via modification of the thin film deposition parameters.

S5. Maximum bending radius of BANN-based TC and comparison with other types of TCs

There have been various types of flexible transparent conductors. As a comparison, maximum bending radius test result is included. The maximum bending radius is under 1 mm considering PET film thickness (0.13 mm) for BANN. Further bending is unattainable since the PET substrate is permanently damaged at 1 mm bending radius. Figure S5 shows superior mechanical property of BANN as compared to other types of flexible transparent conductors.

S6. Long term cyclic test result of BANN-based TC

The effect of bundled wire structure has long been used in the field of structural engineering. The best example can be found in a structural component of typical suspension bridge: the suspension cable which consists of multiple strand of wires. As a strand of wire alone cannot carry much weight, however a bundle of the same wires can withstand much more weight. Similar effect is anticipated from the bundled NWs. The BANN consists of numerous nanowires in a bundle, thus

structural failure of several NWs is not critical to function as a conductor. This can be shown in the maximum bending radius test and long term cyclic test, Figure S5 and Figure S6.

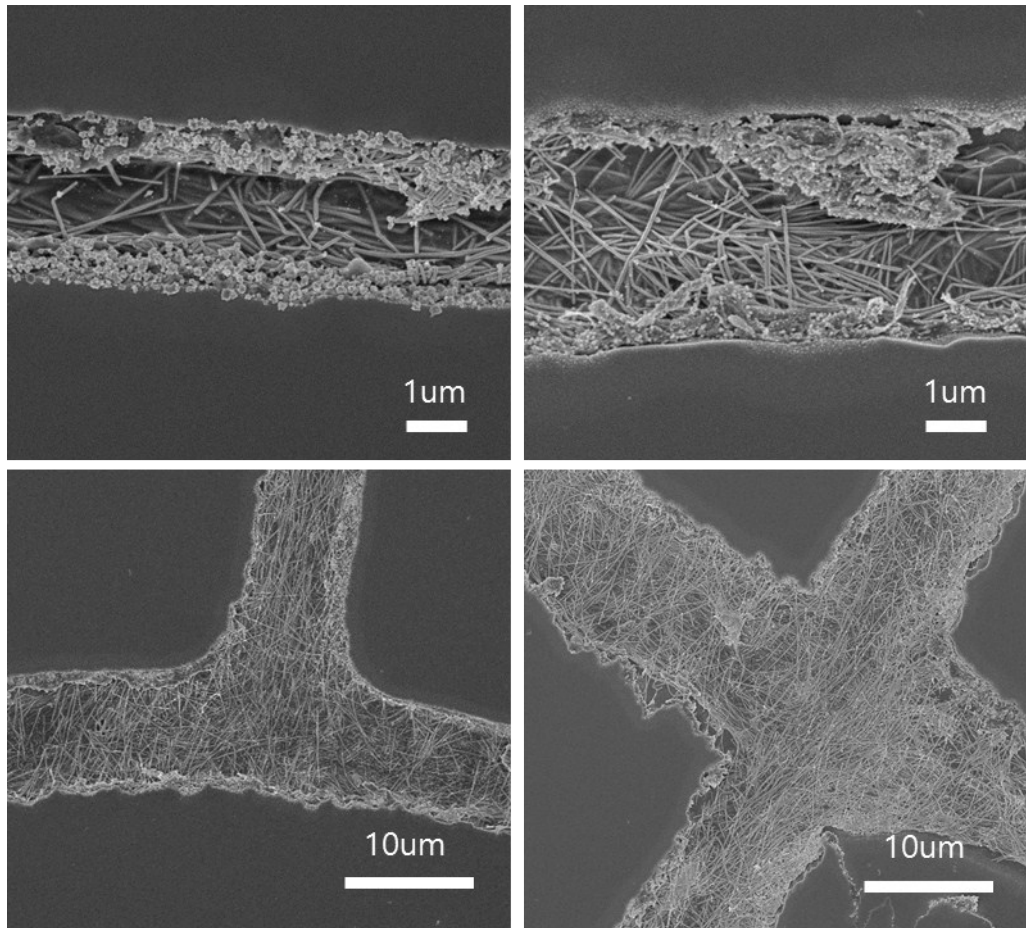


Figure S1. Template patterns filled with AgNWs. Various pattern line width can be controlled by etching time.

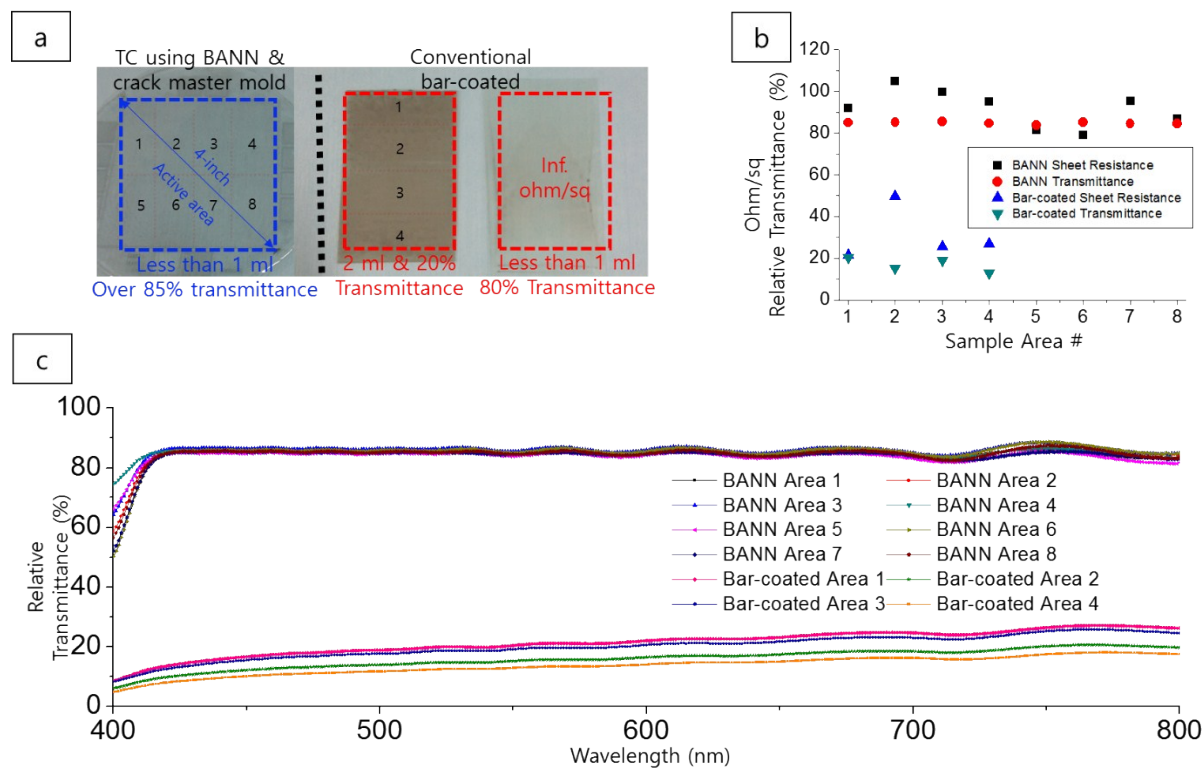


Figure S2. Comparison between bar-coated and BANN based TC. a) TC samples fabricated using BANN (left most) and bar-coating method. b) Relative transmittance at 500 nm wavelength and sheet resistance of TC samples. Notice, bar coated highly transparent sample is omitted due to lack of conductance. c) Relative optical transmittance of TC samples.

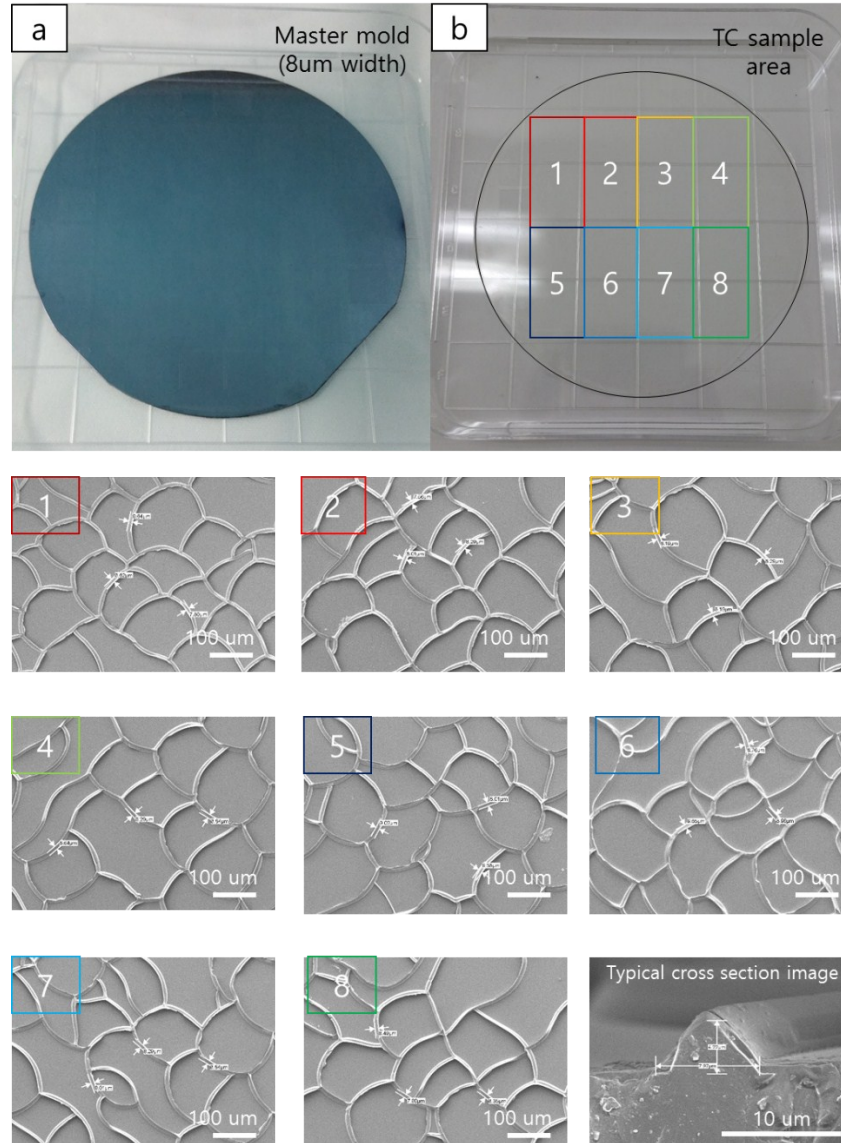


Figure S3. Crack distribution on master mold. a) Image of 4-inch wafer size mater mold. b) Image of replicated master mold. Notice, replica sample is divided into 8-different subsection. c) Images of an arbitrary location of each sections and typical cross section image of inverse mold (bottom right).

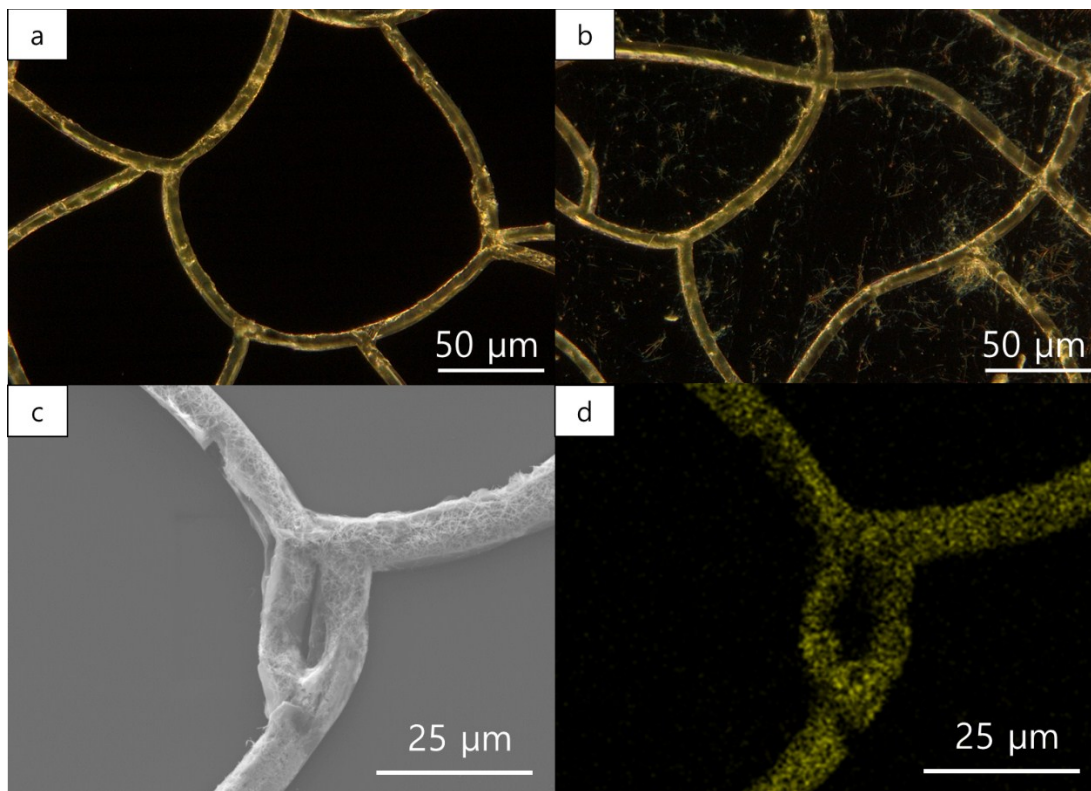


Figure S4. Optical microscope image of (a) clean master mold after additional blading and (b) before scrape off blading. c) SEM image of transferred replica with BANN and d) corresponding EDS image showing Ag peak in yellow color. Notice no residues near BANN.

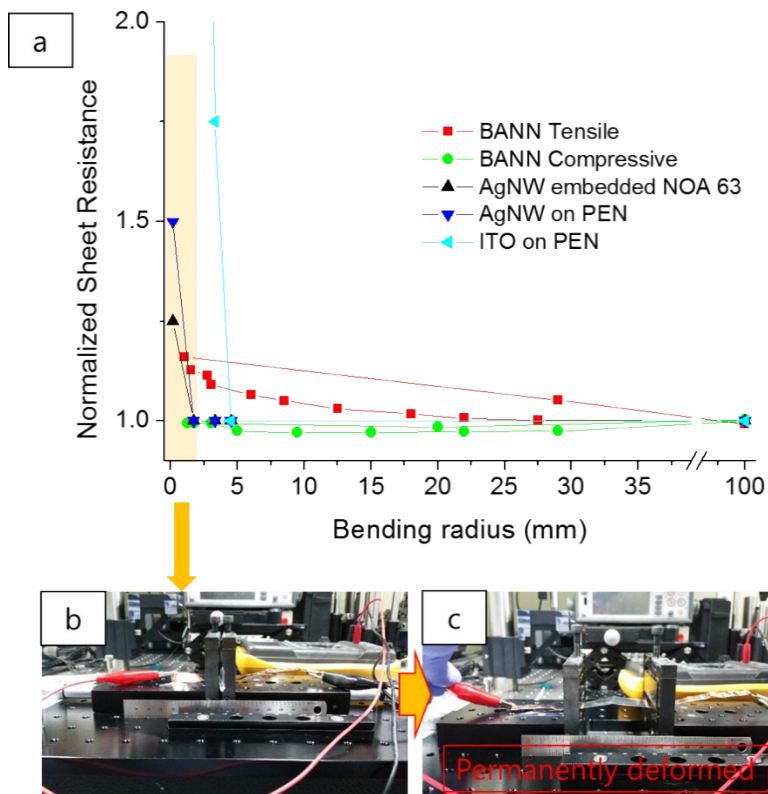


Figure S5. Comparison between different types of TCs (a). (b) and (c) shows maximum bending radius and released TC sample respectively.

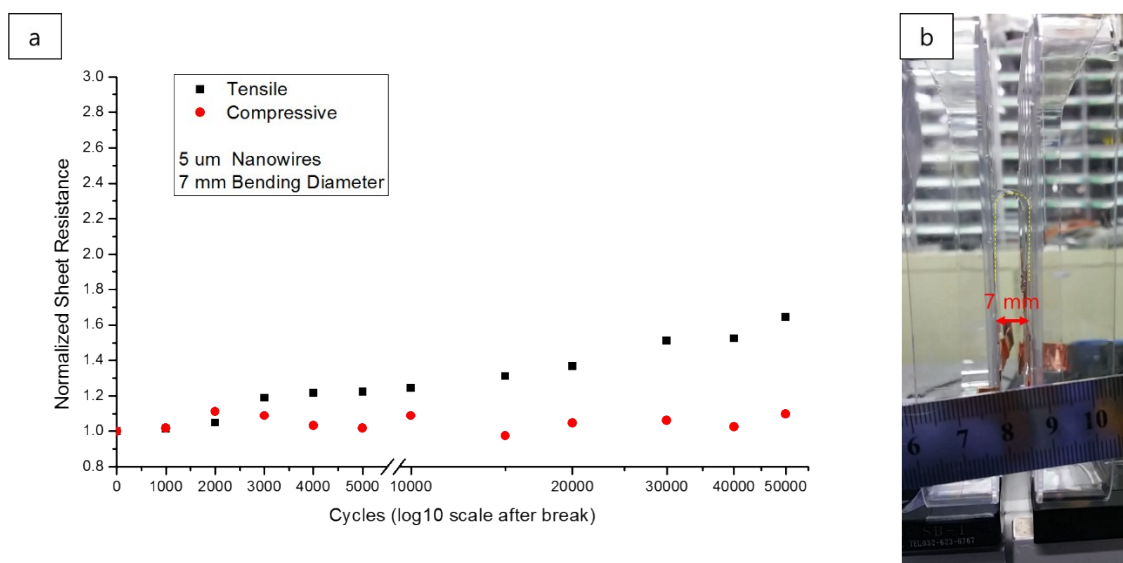


Figure S6. a) Long term mechanical property of BANN. b) Test setup showing maximum 3.5 mm bending radius.